Published in final edited form as:
Eur J Oral Sci. 2013 August ; 121(4): 293–302. doi:10.1111/eos.12059.

Ameloblasts require active RhoA to generate normal dental enamel

Yong Li[1,+], **Hui Xue**[1,+], **Eric T. Everett**[2], **Kathleen Ryan**[3], **Li Peng**[1], **Rakhee Porecha**[1], **Yan Yan**[1], **Anna M. Lucchese**[1], **Melissa A. Kuehl**[1], **Megan K. Pugach**[1,#], **Jessica Bouchard**[1], and **Carolyn W. Gibson**[1]

[1]Department of Anatomy and Cell Biology, University of Pennsylvania School of Dental Medicine, Philadelphia, PA 19104, USA

[2]Department of Pediatric Dentistry, University of North Carolina School of Dentistry, Chapel Hill, NC 27599, USA

[3]Dental Research, University of North Carolina School of Dentistry, Chapel Hill, NC 27599, USA

Abstract

RhoA plays a fundamental role in regulation of the actin cytoskeleton, intercellular attachment and cell proliferation. During amelogenesis, ameloblasts which produce the enamel proteins undergo dramatic cytoskeletal changes and RhoA protein level is upregulated. Transgenic mice were generated that express a dominant-negative RhoA transgene in ameloblasts using amelogenin gene regulatory sequences. Transgenic and WT molar tooth germs were incubated with NaF or NaCl in organ culture. F-actin stained with phalloidin was elevated significantly in WT ameloblasts treated with NaF compared to WT ameloblasts treated with NaCl or compared to transgenic ameloblasts treated with NaF, thereby confirming a block in the RhoA/ROCK pathway in the transgenic mice. Little difference in quantitative fluorescence (estimation of fluorosis) was observed between WT and transgenic incisors from mice provided NaF in their drinking water. We subsequently found reduced transgene expression in incisors compared to molars. Transgenic molar teeth had reduced amelogenin, E-cadherin and Ki67 compared to WT. Hypoplastic enamel in transgenic mice correlates with reduced expression of the enamel protein amelogenin, and E-cadherin and cell proliferation are regulated by RhoA in other tissues. Together these findings reveal deficits in molar ameloblast function when RhoA activity is inhibited.

Keywords

dental enamel; dominant negative RhoA; transgenic mice; ameloblasts

Vertebrate teeth develop during a series of reciprocal interactions between epithelial and mesenchymal cell layers within the unerupted tooth germ (1, 2). A single layer of epithelium differentiates into ameloblast cells, which secrete enamel proteins that mineralize to form the enamel layer on the crown of the tooth.

The morphologies of ameloblasts and their cellular precursors change continuously during the various stages of the ameloblast life cycle, in conjunction with the changing functions of

Corresponding author: Carolyn W. Gibson, PhD, Department of Anatomy and Cell Biology, University of Pennsylvania School of Dental Medicine, 240 S. 40th Street, Philadelphia, PA 19104-6030, USA, cgibson@dental.upenn.edu.
[+]Both authors contributed equally to this research

CONFLICTS OF INTEREST
This work did not involve any conflicts of interest.

these cells (3). Early in development, a layer of short inner enamel epithelium participates in signaling with the underlying dental papilla (1), which ultimately forms the adjacent mineralized dentin layer. The inner enamel epithelium differentiates into tall secretory-stage ameloblasts, which have an actin-rich secretory structure referred to as Tomes' process, from which enamel proteins are released into the developing enamel layer (4). After the full thickness of enamel has been produced, the secretory ameloblasts undergo a transition, in which the cells reorganize to become shorter and Tomes' process retracts. During the subsequent maturation stage, ameloblasts undergo a series of modulations in which the distal cell surface adjacent to the enamel layer changes repeatedly from a smooth appearance to a highly indented or ruffled surface (5). These changes accompany functional alterations in transferring calcium and phosphate into developing enamel and retrieving organic material from the enamel layer to increase mineral content. As the cell reorganizes from a short epithelial cell, to a secretory ameloblast which can be 50 μm in height, to a shorter cell able to alter its apical surface, to finally a protective ameloblast firmly attached to the enamel surface by hemi-desmosomes, the actin cytoskeleton must also continuously reorganize (6, 7).

The RhoA pathway has a fundamental role in regulation of the actin cytoskeleton in both fibroblastic and epithelial cell types (8, 9). RhoA is a well-studied member of the Rho GTPase superfamily of small G proteins, and as a molecular switch cycles between active and inactive forms with regulation that include GAPs (activating proteins) and GEFs (exchange factors; 10, 11). The RhoA downstream effector ROCK (Rho associated protein kinase) when activated increases actin stress fiber formation (12).

Filamentous actin (F-actin) in cultured fibroblasts can be elevated by treatment with high concentrations of sodium fluoride. This occurs by inhibition of RhoGAP activity which activates RhoA, and can be detected microscopically using phalloidin stain of intracellular F-actin (11). We have shown that NaF can also be used as a tool to study F-actin upregulation in ameloblasts of wild-type murine teeth in organ culture, also through the RhoA pathway. The two-fold elevation of F-actin by NaF was diminished in the presence of relatively specific inhibitors of ROCK including Y-27632 and fasudil (HA1077) in tooth organ cultures (13-15), indicating the central role of the RhoA/ROCK pathway in F-actin induction within the ameloblast cytoskeleton.

Because RhoA signals through at least 28 downstream effectors, this small G protein is able to affect diverse cellular activities including intercellular adherens junctions, cell polarity, proliferation and migration, as well as gene expression in various cell types (16). Regulated intercellular attachments are thought to be important for ameloblasts to develop the cross-hatched decussation patterns found in normal enamel (7, 17). E-cadherins have been intensely studied because of their association with adherens junctions of ameloblasts (18-20), and immunolocalization analyses have shown E-cadherins are abundant in presecretory ameloblasts, reduced during secretory stage, elevated during transition and then reduced again during maturation (21,22). Interestingly, the expression is opposite to that of adenomatous polyposis coli (APC) in rat incisors, which is elevated during secretion and maturation (23). RhoA is required for establishment of cadherin binding between cells (24), and treatment of murine incisors in culture with Y27632, the ROCK inhibitor, led to weak, abnormally distributed, E-cadherin immunostaining in ameloblasts (25), thereby further implicating the RhoA pathway in normal activities of ameloblasts.

We and others have shown endogenous RhoA mRNA or protein is abundantly expressed in rodent ameloblasts, increasing from newborn until PN5 (postnatal day 5) in rat molars and until PN8 in murine molars (14, 26, 27). In order to evaluate RhoA function in differentiating ameloblasts *in vivo*, a transgenic approach was developed in which

dominant-negative T19N RhoA (28) was expressed under control of the amelogenin regulatory sequences. This led to a transgene expression pattern similar to the endogenous RhoA and amelogenin genes, with the goal of deregulating activities of the endogenous RhoA protein during ameloblast secretory stage. The expression vector was planned so that $RhoA^{DN}$ was fused to the EGFP reporter protein, allowing expression to be localized using immunohistochemistry to GFP. Others have shown that $RhoA^{DN}$ is active when fused to EGFP and that the T19N dominant negative RhoA has activity in rodents *in vivo* (29-31).

We hypothesized that interference with the RhoA pathway *in vivo* would lead to defective dental enamel structure, and we have observed that the EGFP-$RhoA^{DN}$ transgenic mice develop a molar defect, where enamel is hypoplastic and disorganized at the cuspal surface (15). Because not only ROCK but also other downstream RhoA effectors are predicted to be affected, these transgenic mice have been analyzed to better explain the mechanism behind the enamel defect.

MATERIAL AND METHODS

Molecular analysis of EGFP-$RhoA^{DN}$ transgenic mice

Genomic DNA from tail tissue was analyzed by PCR from the three strains TgEGFP-$RhoA^{DN}$-2, 8 and 13 as described (15). The transgene is regulated by amelogenin gene sequences to target expression to ameloblasts. All work was performed in accordance with regulations of the University of Pennsylvania Institutional Animal Care and Use Committee.

Organ culture and phalloidin staining

Dissected first mandibular molars from postnatal day 2 (PN2) transgenic or wild-type (WT) mice were placed into organ culture and treated as described previously (14). Briefly, teeth were incubated in BGJb medium (Gibco/Invitrogen, Carlsbad, CA, USA) containing 10% fetal bovine serum with 50 μg/ml ascorbic acid to reduce toxicity. NaF or NaCl was added to 4 mM final concentration for left or right first molars from each mouse for 30 min at 37°C. Tooth germs were immediately fixed with 4% paraformaldehyde overnight, embedded in OCT (Tissue-Tek, Torrance, CA, USA), sectioned using a cryostat and stained with phalloidin AlexaFluor 546 as described (14). Slides were photographed and images were analyzed using ImageJ software (http://rsb.info.nih.gov/ij/).

Measurement of dental fluorosis by quantitative fluorescence

WT and TgEGFP-$RhoA^{DN}$-13 transgenic mice were provided 0, 50 or 100 ppm F ion in drinking water as NaF for 4 weeks *ad libitum* beginning at PN21 (n = 6 for each group). Mice were then euthanized and heads were frozen until analysis.

For the clinical examination, a single examiner (ETE) performed duplicate evaluations of dental fluorosis status for each animal. The determination of dental fluorosis was made clinically over the entire lower incisor tooth surfaces according to a modified Thylstrup & Fejerskov (TF) index (32-37).

A quantitative fluorescence (QF) system was previously devised to evaluate the severity of fluorosis in mice (32, 34, 38, 39). A Nikon epifluorescence microscope equipped with a Chroma Gold 11006v2 set cube (exciter D360/40x, dichroic 400DCLP, and emitter E515LPv2) was used to capture fluorescent images of teeth. The lower incisors were removed from the mandible and allowed to remain slightly moist. Teeth were viewed, labial side up and flat, on a black background at 2X magnification. Eleven-megapixel Bmp images were acquired under standard exposure conditions. Images were analyzed with Image J software version 1.33u (http://rsb.info/nih.gov/ij/). Briefly, ten 300 × 300 pixel areas were

randomly positioned over the pair of lower incisors and the mean grayscale values for each square determined. The average grayscale values for all 10 regions were then determined.

Measurement of elastic modulus and hardness

Elastic modulus and hardness of molar enamel were determined in 8 wk-old WT and transgenic mice (n=6) by a Nanoindenter XP (MTS Systems, Oak Ridge, TN, USA). Half-mandibles were embedded in Acrymount embedding resin (Electron Microscopy Sciences, Hatfield, PA, USA) and polished mesial-distally with 400-grit silicon carbide paper to reveal longitudinal cross-sections of molars, perpendicular to the orientation of enamel prisms. Embedded mandibles were further polished to 0.25 μm with diamond paste. Nano-indentations were performed with a Berkovich diamond tip, under dry conditions, with a trapezoidal force profile with peak loads at 300 μN. Twenty indentations were made in the enamel of each tooth in mesial cusps of first molars. Each indentation yielded a load-deformation curve, from which the elastic modulus, E, and hardness, H, were determined according to the following equations (40):

$$E=\sqrt{\pi}/2\sqrt{a} \bullet S$$
$$H=Fmax/a$$

where S represents the slope of the unloading curve based on the method of Oliver & Pharr (41), *a* is the indentation contact area, and Fmax is the maximum force.

Immunohistochemistry

Mandibles dissected from PN 1-8 WT and TgEGFP-RhoA^{DN}-13 mice were fixed in 4% paraformaldehyde, demineralized in 5% EDTA when necessary and embedded in paraffin. One 5 μm section was stained with hematoxylin and eosin (H&E), and other sections were incubated with peroxide in PBS followed by anti-GFP (Ab6556, Abcam, Cambridge, MA, USA). An adjacent control section was incubated without primary antibody. After washing, the sections were incubated with secondary antibody (Vectastain ABC kit PK-4001, Vector Laboratories, Burlingame, CA, USA) and DAB substrate (Vector Laboratories). WT and transgene negative mice served as negative controls.

Immunohistochemistry studies for E-cadherin and Ki67 were performed similarly using 1:200 dilution of anti-E-cadherin (24E10, Cell Signaling Technology, Danvers, MA, USA) or 1:5000 of anti-Ki67 (ab15580) (Abcam) followed by the Vectastain procedures described above.

Western blots

Two mandibular first molar teeth from PN4 pups of WT and each transgenic strain were dissected and proteins were extracted; blots were prepared as described (42). Membranes were incubated with anti-GFP antibody (Ab6556, Abcam) at 1:1000 dilution and goat anti-rabbit secondary antibody (Thermo-Fisher, Rockford, IL, USA) at 1:2000 dilution. Additional membranes were probed with anti-RhoA (67B9#2117, Cell Signaling Technology) at 1:1000 dilution and goat anti-rabbit antibody, and reprobed without stripping with anti-actin antibody (A2103, Sigma, St. Louis, MO, USA). Western blots were prepared similarly to compare molar and incisor transgene expression, except 10 μg was loaded onto each lane of the gel.

For detection of amelogenin, anti-amelogenin (Santa Cruz Biotechnology, Santa Cruz, CA, USA) and anti-GAPDH (Cell Signaling Technology) at 1:1000 dilution were used with enamel organ extracts as described (27). Bands were scanned for normalization using

ImageJ software (43). For the Western blot of transgenic protein amounts in mandibular first molars and incisors, 10 μg of extract from each tooth type from PN4 mice was compared using anti-GFP antibody as described above.

Statistics

Statistical significance was assessed using ANOVA with Bonferroni's multiple comparison test, with significance defined as $P<0.05$ (GraphPad Prism 5, Graph Pad Software, San Diego, CA, USA).

RESULTS

Three founders were generated that express RhoA^{DN}

Three founder mice identified by PCR of tail genomic DNA were mated with C57BL/6J WT mice to generate independent strains, TgEGFP-RhoA^{DN}-2, -8 and -13. In order to compare transgene expression among the three strains, extracts of molar teeth were prepared for SDS-PAGE, including transgene negative, WT and transgene positive molars. The Western blots probed with anti-RhoA antibody identified the EGFP-RhoA^{DN} fusion protein at 48 kDa in the three transgenic strains plus the endogenous RhoA protein visible at 22 kDa for all mice (Fig. 1). Blots were also probed for GFP, and the antibody detected the identical transgenic fusion protein at 55-60 kDa in the 3 transgenic extracts (not shown). Membranes were re-probed with anti-actin antibody for normalization. Quantitation indicated that strain TgEGFP-RhoA^{DN}-13 had the highest expression, strain -8 had the lowest and strain -2 was intermediate.

RhoA^{DN} expression during molar development

Transgenic and WT mandibles were also prepared for reporter protein localization. Immunohistochemistry using anti-GFP antibodies revealed staining of the ameloblast layer beginning at PN2 which became intense at PN3 and PN4 (Fig. 2A-D). Expression decreased at molar cusp tips at PN6 and localized only to the cervical loop region by PN8 (Fig. 2E,F), in agreement with Western analysis (27). Staining was negligible when primary antibody was omitted.

Organ culture revealed the dominant negative effects of the transgene

In order to determine whether the dominant negative transgene could inhibit F-actin elevation by NaF, first molar tooth germs were dissected and placed into organ culture in the presence of 4 mM NaF or NaCl. For all three strains, RhoA activity was indirectly assessed under identical conditions by phalloidin staining of ameloblast F-actin, by generating images of the ameloblasts under fluorescent microscopy (14, 15). WT molars treated with NaF had greater phalloidin staining intensity in ameloblasts compared to WT ameloblasts in molars treated with NaCl ($P<0.0001$), or in molar ameloblasts from each transgenic strain treated with NaF ($P<0.0001$), consistent with the block to the RhoA pathway in the three transgenic strains (Fig. 3).

For subsequent studies, the TgEGFP-RhoA^{DN}-13 (referred to as E13) mice were used due to the higher transgene expression level, as we are unable to precisely measure the amount of dominant negative activity required for an informative phenotype to develop.

Quantitative fluorescence

WT and transgenic mice were given NaF in their drinking water in order to determine whether the dominant negative RhoA could alter the fluorotic phenotype in incisor enamel. WT and TgEGFP-RhoA^{DN}-13 mice were given 0, 50 or 100 ppm F ion as NaF in their

drinking water for 4 wk. The clinical images of an example of each treatment and genotype are shown in Fig. 4. In the mandibular incisors and less so in the maxillary incisors, dental fluorosis developed similarly when comparing WT and TgEGFP-Rho^{DN}-13 mice. Quantitative fluorescence (QF) results in Fig. 5 show a dose dependent increase in dental fluorosis for WT and TgEGFP-RhoA^{DN}-13 mice. QF was significantly different comparing WT and transgenic incisor controls (0 ppm) to 100 ppm [F-] ($P<0.001$), but no statistically significant differences were observed between WT and TgEGFP-RhoA^{DN} mice treated at 0ppm or 100ppm [F-]. However, at 50 ppm, QF was higher for TgEGFP-RhoA^{DN} mice compared to WT ($P<0.05$).

To better understand why WT and transgenic mice treated with 100 ppm F- had similar QF values for incisors, we questioned whether the transgene was expressed at a lower level in incisors compared to molars. Western blots indicated elevated transgene expression in molars compared to incisors (Fig. 6) consistent with the QF results described above, although RT-PCR detected a low transgene expression in incisors. The reduction in incisor expression was greater than observed with other transgenic mice based on this vector system (42, 44). Subsequent transgenic studies focused on the developing molar.

Structural properties of enamel

Transgenic molar enamel elastic modulus trended somewhat lower and nanohardness somewhat higher compared to WT, but these differences were not statistically significant (Table 1). These nanoindentation measurements were made on cross sections of molar teeth from the enamel surface and ending at the dentin-enamel junction, as described in Material and Methods.

Ameloblasts are altered in transgenic mice

By Western analysis, amelogenin proteins were reduced in transgenic molar enamel organs compared with WT, with statistical significance ($P<0.001$) at PN2 and 4 (Fig. 7A-C). This is in agreement with the observed enamel hypoplasia in these transgenic mice, as reduced amelogenin also led to enamel hypoplasia in molars from amelogenin null or partially rescued mice (42, 45).

Immunohistochemistry for ameloblast E-cadherin invariably showed less staining in transgenic mandibular or maxillary molars compared to WT molars from mice of identical age and weight (Fig. 8A-E). These comparisons were performed with six independent pairs of age/weight matched mice with similar results. In addition, a difference was observed in Ki67 immunostaining at PN2-3, which is an indicator of cells undergoing DNA synthesis, linked with cell proliferation (46). In each set of paired samples, WT molars had more positive presecretory ameloblasts than transgenic molars (Fig. 9A-E).

DISCUSSION

The RhoA pathway is critical for dynamic re-organization of the actin cytoskeleton and ameloblasts are unique in that their cell shapes continually change during their life cycle and these morphological changes are linked with functional changes. RhoA protein is induced during differentiation of WT murine ameloblasts, and the Rho inhibitor RhoGDI normally decreases in ameloblasts as enamel protein expression begins, presumably to direct RhoA activation (47). To test the importance of the RhoA pathway during enamel formation, we generated mice that express RhoA^{DN} protein in secretory ameloblasts during enamel development. The dominant negative T19N mutation allows binding to RhoGEFs, but reduces downstream target interactions (48).

Previously, cultured fibroblasts had been treated with NaF, which interferes with RhoGAP and elevates RhoA activity (11), and F-actin was increased. Similarly, in tooth germs treated with NaF in organ culture and stained with phalloidin, F-actin was visualized by confocal microscopy and a doubling of F-actin was measured in WT ameloblasts (14). The increase in F-actin was reduced by Y-27632 or fasudil (HA1077) (14, 15), inhibitors of the RhoA downstream target ROCK (12). We hypothesized that RhoA also has a role during normal enamel development related to regulation of ameloblast activities.

Three transgenic lines of mice are described in which $RhoA^{DN}$ was expressed at different levels in molar ameloblasts. The molar tooth germs from each strain were placed into organ culture as described above with NaF or NaCl, and while the WT ameloblasts had elevated F-actin in the presence of NaF, the transgenic ameloblasts had no increase. This illustrated the dominant negative block to F-actin induction in the transgenic mice, similar to results shown in the presence of NaF plus ROCK inhibitors in WT ameloblasts in organ culture.

An enamel surface defect is present prior to molar eruption in these transgenic mice, and all 3 transgenic strains have hypoplastic molar enamel (42). Previously, we reported that the transgene was highly expressed in molars at PN4, but decreased at PN8, as expected due to regulation by amelogenin gene sequences. ROCK activity was elevated at PN6 and PN8 in WT mice, but reduced to less than half the WT level in TgEGFP-$RhoA^{DN}$-13 ameloblasts (27). Because the QF results presented here led us to ascertain that molars expressed higher levels of transgene than incisors, and that molar expression begins by PN2 and is elevated on PN3 and PN4, transgene expression in this mouse model would be expected to have impacts on events primarily during molar secretory stage. The elevated QF results for incisors of transgenic mice treated with 50 ppm F- were surprising; future experimentation may lead to a better understanding of this finding.

Amelogenins are the principal enamel proteins expressed during the secretory stage of ameloblasts (49). TgEGFP-$RhoA^{DN}$-13 mice have significantly reduced amelogenin during secretory stage when the $RhoA^{DN}$ transgene expression is elevated, and at 8 weeks of age, mice have enamel hypoplasia (15). When developing WT teeth were incubated with ROCK inhibitor Y-27632, amelogenin mRNA and protein were both reduced (25, 26). Together, these findings strengthen the conclusion that RhoA pathway elements can regulate aspects of enamel development.

RhoA signaling elevates filamentous actin (F-actin), which is localized primarily to ameloblast intercellular binding sites and Tomes' process (6). Adherens junctions are linked to actin filaments and thought to participate in cellular interactions that generate sliding rows of ameloblasts during development, leading to unique enamel decussation patterns (7, 3). Cadherin levels normally decrease and increase cyclically during incisor ameloblast differentiation presumably to allow efficient cellular reorganization (19, 22). β-catenin is also linked to adherens junctions, and was previously shown to be elevated in PN4 transgenic molar ameloblasts (43). Although associated with junctional complexes, β-catenin also can migrate to the nucleus to direct gene transcription (50). This elevation of β-catenin in the transgenic ameloblasts may be linked to activation of Wnt pathway elements, known to be important during normal tooth development (27, 51).

Cellular polarity was unaffected in transgenic ameloblasts, perhaps because by the time transgene expression was elevated, intercellular contacts had been firmly established. The decrease in Ki67 positive cells also would indicate that polarity could be established early in the transgenic mice. Over-expressed RhoA elevates proliferation and migration of tumor cells while siRNA mediated reduction in RhoA inhibits both activities (52, 53). Inactivation of RhoA can lead to increase or inhibition of cell proliferation in different cell types (54,

55). Reduction in endogenous RhoA by various means has been associated with weakening of the cadherin-based contacts in other models (24, 55, 56), which may explain lower E-cadherin levels observed by immunohistochemistry in transgenic ameloblasts compared to WT. The structural alterations at tips of molar cusps in transgenic mice correspond to expression during mid to late secretory stage, and it is assumed that enamel secretion was altered prior to PN8 when transgene expression was again reduced and cells entered maturation stage (15).

In summary, we provide further support that RhoA has a role in generation of a normal enamel layer by ameloblasts. We show that in the presence of a dominant negative RhoA, amelogenin protein was reduced, which correlates with hypoplastic enamel. Expression of the transgene led to reduction in RhoA/ROCK activity, and elevated β-catenin levels previously noted (27) were also temporally linked with reduced E-cadherin and reduced DNA synthesis in ameloblasts. E-cadherin, p120 catenin, β-catenin and ROCK are components of adherens junctions (24, 57-59), which are intercellular attachment sites, thought to be critically important for the precise dynamic alterations between ameloblasts during generation of the decussating enamel rod patterns found in mature enamel of erupted teeth. We predict that these mice will provide a valuable tool to further dissect the role of the RhoA pathway during amelogenesis as they present a phenotype linked to critical events occurring during several days of the ameloblast secretory stage when the transgene is highly expressed.

Acknowledgments

We acknowledge the University of Pennsylvania Transgenic Core Facility for generation of transgenic mice and the School of Dental Medicine vivarium personnel for animal husbandry. We thank K. Jordan-Sciutto, C. Robinson, Y. Takano, S. Nishikawa, T. Bromage for scientific insights, and Z. Nikolov from the Centralized Research Facilities in the College of Engineering at Drexel University, for assistance with nanoindentation training. This work was supported by the National Institutes of Health through grants R21-DE017610 and DE011089 (CWG), F32-DE019968 (MKP), DE018104 (ETE), and the Cheung Family Scholarship (LP). Strain 13 transgenic mice have been deposited with the MMRRC (Bar Harbor, ME, USA) and designated B6;SJL-Tg(EGFP-RhoADN)13Gibs/Mmjax, with stock number 036752.

References

1. THESLEFF I, SHARPE P. Signaling networks regulating dental development. Mech Dev. 1997; 67:111–123. [PubMed: 9392510]
2. JERNVALL J, THESLEFF I. Reiterative signaling and patterning during mammalian tooth morphogenesis. Mech Dev. 2000; 92:19–29. [PubMed: 10704885]
3. SMITH CE, NANCI A. Overview of morphological changes in enamel organ cells associated with major events in amelogenesis. Int J Dev Biol. 1995; 39:153–161. [PubMed: 7626402]
4. SMITH CE. Ameloblasts: secretory and resorptive functions. J Dent Res. 1979; 58(Spec Issue B): 695–707. [PubMed: 283112]
5. SMITH CE. Cellular and chemical events during enamel maturation. Crit Rev Oral Biol Med. 1998; 9:128–161. [PubMed: 9603233]
6. NISHIKAWA S, KITAMURA H. Localization of actin during differentiation of the ameloblast, its related epithelial cells and odontoblasts in the rat incisor using NBD-phallacidin. Differentiation. 1986; 30:237–243. [PubMed: 3699311]
7. NISHIKAWA S, FUJIWARA K, KITAMURA H. Formation of the tooth enamel rod pattern and the cytoskeletal organization in secretory ameloblasts of the rat incisor. Eur J Cell Biol. 1988; 47:222–232. [PubMed: 3149586]
8. RIDLEY AJ, HALL A. The small GTP-binding protein rho regulates the assembly of focal adhestions and actin stress fibers in response to growth factors. Cell. 1992; 70:389–399. [PubMed: 1643657]

9. VAN AELST L, SYMONS M. Role of rho family GTPases in epithelial morphogenesis. Genes Dev. 2002; 16:1032–1054. [PubMed: 12000787]
10. LAMARCHE N, HALL A. GAPs for rho-related GTPases. Trends Genetics. 1994; 10:436–440.
11. VINCENT S, SETTLEMAN J. Inhibition of RhoGAP activity is sufficient for the induction of Rho-mediated actin reorganization. Eur J Cell Biol. 1999; 78:539–548. [PubMed: 10494860]
12. MAEKAWA M, ISHIZAKI T, BOKU S, WATANABE N, FUJITA A, IWAMATSU A, et al. Signaling from Rho to the actin cytoskeleton through protein kinases ROCK and LIM-kinase. Science. 1999; 285:895–898. [PubMed: 10436159]
13. DAVIES SP, REDDY H, CAIVANO M, COHEN P. Specificity and mechanism of action of some commonly used protein kinase inhibitors. Biochem J. 2000; 351:95–105. [PubMed: 10998351]
14. LI Y, DECKER S, YUAN ZA, DENBESTEN PK, ARAGON MA, JORDAN-SCIUTTO K, ABRAMS WR, HUH J, MCDONALD C, CHEN E, MACDOUGALL M, GIBSON CW. Effects of sodium fluoride on the actin cytoskeleton of murine ameloblasts. Arch Oral Biol. 2005; 50:681–688. [PubMed: 15958199]
15. LI Y, PUGACH MK, KUEHL MA, PENG L, BOUCHARD J, HWANG SY, GIBSON CW. Dental enamel structure is altered by expression of dominant negative RhoA in ameloblasts. Cells Tiss Organs. 2011; 194:227–231.
16. KHER SS, WORTHYLAKE RA. Nuanced junctional RhoA activity. Nat Cell Biol. 2012; 14:784–786. [PubMed: 22854811]
17. NISHIKAWA S. Correlation of the arrangement pattern of enamel rods and secretory ameloblasts in pig and monkey teeth: a possible role of the terminal webs in ameloblast movement during secretion. Anat Rec. 1992; 232:466–478. [PubMed: 1554099]
18. PALACIOS J, BENITO N, BERRAQUERO R, PIZARRO A, CANO A, GAMALLO C. Differential spatiotemporal expression of E- and P-cadherin during mouse tooth development. Int J Dev Biol. 1995; 39:663–666. [PubMed: 8619966]
19. OBARA N, SUZUKI Y, NAGAI Y, TAKEDA M. Expression of E- and P-cadherin during tooth morphogenesis and cytodifferentiation of ameloblasts. Anat Embryol. 1998; 197:469–475. [PubMed: 9682977]
20. TERLING C, HEYMANN R, ROZELL B, OBRINK B, WROBLEWSKI J. Dynamic expression of E-cadherin in ameloblasts and cementoblasts in mice. Eur J Oral Sci. 1998; 106(suppl 1):137–142. [PubMed: 9541216]
21. FAUSSER J-L, SCHLEPP O, ABERDAM D, MENEGUZZI G, RUCH JV, LESOT H. Localization of antigens associated with adherens junctions, desmosomes, and hemidesmosomes during murine molar morphogenesis. Differentiation. 1998; 63:1–11. [PubMed: 9615388]
22. SORKIN BC, WANG MY, DOBECK JM, ALBERGO KL, SKOBE Z. The cadherin-catenin complex is expressed alternately with the adenomatous polyposis coli protein during rat incisor amelogenesis. J Histochem Cytochem. 2000; 48:397–406. [PubMed: 10681393]
23. WANG M, DOBECK JM, SORKIN BC, SKOBE Z. Adenomatous polyposis coli protein is expressed in alternate stages of the ameloblast life cycle. J Dent Res. 1998; 77:1979–1982. [PubMed: 9839785]
24. BRAGA VMM, MACHESKY LM, HALL A, HOTCHIN NA. The small GTPases Rho and Rac are required for the establishment of cadherin-dependent cell-cell contacts. J Cell Biol. 1997; 137:1421–1431. [PubMed: 9182672]
25. OTSU K, KISHIGAMI R, FUJIWARA N, ISHIZEKI K, HARADA H. Functional role of Rho-kinase in ameloblast differentiation. J Cell Physiol. 2010; 226:2527–2534. [PubMed: 21792909]
26. BIZ MT, MARQUES R, CREMA VO, MORISCOT AS, DOS SANTOS MF. GTPases RhoA and Rac1 are important for amelogenin and DSPP expression during differentiation of ameloblasts and odontoblasts. Cell Tissue Res. 2010; 340:459–470. [PubMed: 20387077]
27. PENG L, LI Y, SHUSTERMAN K, KUEHL M, GIBSON CW. Wnt-RhoA signaling is involved in dental enamel development. Eur J Oral Sci. 2011; 119(Suppl. 1):41–49. [PubMed: 22243225]
28. SUBAUSTE MC, VON HERRATH M, BENARD V, CHAMBERLAIN CE, CHUANG TH, CHU K, BOKOCH GM, HAHN KM. Rho family proteins modulate rapid apoptosis induced by cytotoxic T lymphocytes and Fas. J Biol Chem. 2000; 275:9725–9733. [PubMed: 10734125]

29. MASSOUMI R, LARSSON C, SJOLANDER A. Leukotriene D4 induces stress-fibre formation in intestinal epithelial cells via activation of RhoA and PKCdelta. J Cell Sci. 2002; 115:3509–3515. [PubMed: 12154081]
30. SMITH PG, ROY C, ZHANG YN, CHAUDURI S. Mechanical stress increases RhoA activation in airway smooth muscle cells. Am J Respir Cell Mol Biol. 2003; 28:436–442. [PubMed: 12654632]
31. CHITALEY K, BIVALACQUA TJ, CHAMPION HC, USTA MF, HELLSTRON WJG, MILLS TM, WEBB RC. Biochem Biophys Res Comm. 2002; 298:427–432. [PubMed: 12413959]
32. EVERETT ET, MCHENRY MA, REYNOLDS N, EGGERTSSON H, SULLIVAN J, KANTMANN C, MARTINEZ-MIER JM, STOOKEY GK. Dental fluorosis: variability among different inbred mouse strains. J Dent Res. 2002; 81:794–798. [PubMed: 12407097]
33. EVERETT ET, YAN D, WEAVER M, LIU L, FOROUD T, MARTINEZ-MIER EA. Detection of Dental Fluorosis-Associated Quantitative Trait Loci on Mouse Chromosomes 2 and 11. Cells Tissues Organs. 2009; 189:212–218. [PubMed: 18701810]
34. EVERETT ET. Fluoride's effects on the formation of teeth and bones, and the influence of genetics. J Dent Res. 2011; 90:552–560. [PubMed: 20929720]
35. FEJERSKOV O, LARSEN MJ, RICHARDS A, BAELUM V. Dental tissue effects of fluoride. Adv Dent Res. 1994; 8:15–31. [PubMed: 7993557]
36. THYLSTRUP A, FEJERSKOV O. Clinical appearance of dental fluorosis in permanent teeth in relation to histologic changes. Community Dent Oral Epidemiol. 1978; 6:315–328. [PubMed: 282114]
37. YAN D, WILLETT TL, GU XM, MARTINEZ-MIER EA, SARDONE L, MCSHANE L, GRYNPAS M, EVERETT ET. Phenotypic variation of fluoride responses between inbred strains of mice. Cells Tissues Organs. 2011; 194:261–267. [PubMed: 21555858]
38. CARVALHO JG, LEITE AL, YAN D, EVERETT ET, WHITFORD GM, BUZALAF MA. Influence of genetic background on fluoride metabolism in mice. J Dent Res. 2009; 88:1054–1058. [PubMed: 19828896]
39. SHARMA R, TYE CE, ARUN A, MACDONALD D, CHATTERJEE A, ABRAZINSKI T, EVERETT ET, WHITFORD GM, BARTLETT JD. Assessment of dental fluorosis in Mmp20 +/- mice. J Dent Res. 2011; 90:788–792. [PubMed: 21386097]
40. DOERNER MF, NIX WD. A method for interpreting the data from depth-sensing indentation instruments. J Mater Res. 1986; 1:601–609.
41. OLIVER WC, PHARR GM. An improved technique for determining hardness and elastic modulus using load and displacement sensing indentation experiments. J Mater Res. 1992; 7:1564–1583.
42. LI Y, SUGGS C, WRIGHT JT, YUAN ZA, ARAGON M, FONG H, SIMMONS D, DALY B, GOLUB EE, HARRISON G, KULKARNI AB, GIBSON CW. Partial rescue of the amelogenin null dental enamel phenotype. J Biol Chem. 2008; 283:15056–15062. [PubMed: 18390542]
43. RASBAND, WS. ImageJ. US National Institutes of Health; Bethesda, MD: 1997-2009. http://rsb.info.nih.gov/ij/
44. PUGACH MK, LI Y, SUGGS C, WRIGHT JT, ARAGON MA, YUAN ZA, SIMMONS D, KULKARNI AB, GIBSON CW. The amelogenin C-terminus is required for enamel development. J Dent Res. 2010; 89:165–169. [PubMed: 20042744]
45. GIBSON CW, YUAN ZA, HALL B, LONGENECKER G, CHEN E, THYAGARAJAN T, SREENATH T, WRIGHT JT, DECKER S, PIDDINGTON R, HARRISON G, KULKARNI AB. Amelogenin-deficient mice display an amelogenesis imperfect phenotype. J Biol Chem. 2001; 276:31871–31875. [PubMed: 11406633]
46. ENDL E, GERDES J. Posttranslational modifications of the KI-67 protein coincide with two major checkpoints during mitosis. J Cell Physiol. 2000; 182:371–380. [PubMed: 10653604]
47. HATAKEYAMA J, FUKUMOTO S, NAKAMURA T, HARUYAMA N, SUZUKI S, HATAKEYAMA Y, SHUM L, GIBSON CW, YAMADA Y, KULKARNI AB. Synergistic roles of amelogenin and ameloblastin. J Dent Res. 2009; 88:318–322. [PubMed: 19407150]
48. HEASMAN SJ, RIDLEY AJ. Mammalian Rho GTPases: new insights into their functions from in vivo studies. Nat Rev Mol Cell Biol. 2008; 9:690–701. [PubMed: 18719708]

49. TERMINE JD, BELCOURT AB, CHRISTNER PJ, CONN KM, NYLEN MU. Properties of dissociatively extracted fetal tooth matrix proteins. I. Principal molecular species in developing bovine enamel. J Biol Chem. 1980; 255:9760–9768. [PubMed: 7430099]
50. CLEVERS H. Wnt/β-catenin signaling in development and disease. Cell. 2006; 127:469–480. [PubMed: 17081971]
51. LIU F, MILLAR SE. Wnt/β-catenin signaling in oral tissue development and disease. J Dent Res. 2010; 89:318–330. [PubMed: 20200414]
52. PILLE JY, DENOYELLE C, VARET J, BERTRAND JR, SORIA J, OPOLON P, LU H, PRITCHARD LL, VANNIER JP, MALVY C, SORIA C, LI H. Anti-RhoA and anti-RhoC siRAs inhibit the proliferation and invasiveness of MDA-MB-231 breast cancer cells in vitro and in vivo. Mol Ther. 2005; 11:267–274. [PubMed: 15668138]
53. GOU L, WANG W, TONG A, YAO Y, ZHOU Y, YI C, YANG J. Proteomic identification of RhoA as a potential biomarker for proliferation and metastasis in hepatocellular carcinoma. J Mol Med(Berl). 2011; 89:817–827. [PubMed: 21475975]
54. TAKEDA N, KONDO M, ITO S, ITO Y, SHIMOKAWA K, KUME H. Role of RhoA inactivation in reduced cell proliferation of human airway smooth muscle by simvastatin. Am J Respir Cell Mol Biol. 2006; 35:722–729. [PubMed: 16858009]
55. KATAYAMA K, MELENDEZ J, BAUMANN JM, LESLIE JR, CHAUHAN BK, NEMKUL N, LANG RA, KUAN CY, ZHENG Y, YOSHIDA Y. Loss of RhoA in neural progenitor cells causes the disruption of adherens junctions and hyperproliferation. Proc Natl Acad Sci USA. 2011; 108:7607–7612. [PubMed: 21502507]
56. WATANABE T, SATO K, KAIBUCHI K. Cadherin-mediated intercellular adhesion and signaling cascades involving small GTPases. Cold Spring Harb Perspect Biol. 2009; 1:a003020. [PubMed: 20066109]
57. WEIS WI, NELSON WJ. Re-solving the cadherin-catenin-actin conundrum. J Biol Chem. 2006; 281:35593–35597. [PubMed: 17005550]
58. BARTLETT JD, DOBECK JM, TYE CE, PEREZ-MORENO M, STOKES N, REYNOLDS AB, FUCHS E, SKOBE Z. Targeted p120-catenin ablation disrupts dental enamel development. PLOS One. 2010; 5:e12703. doi:10, 1371/journal.pone.0012703. [PubMed: 20862276]
59. SMITH AL, DOHN MR, BROWN MV, REYNOLDS AB. Association of Rhoassociated protein kinase 1 with E-cadherin complexes is mediated by p120-catenin. Mol Biol Cell. 2012; 23:99–110. [PubMed: 22031287]

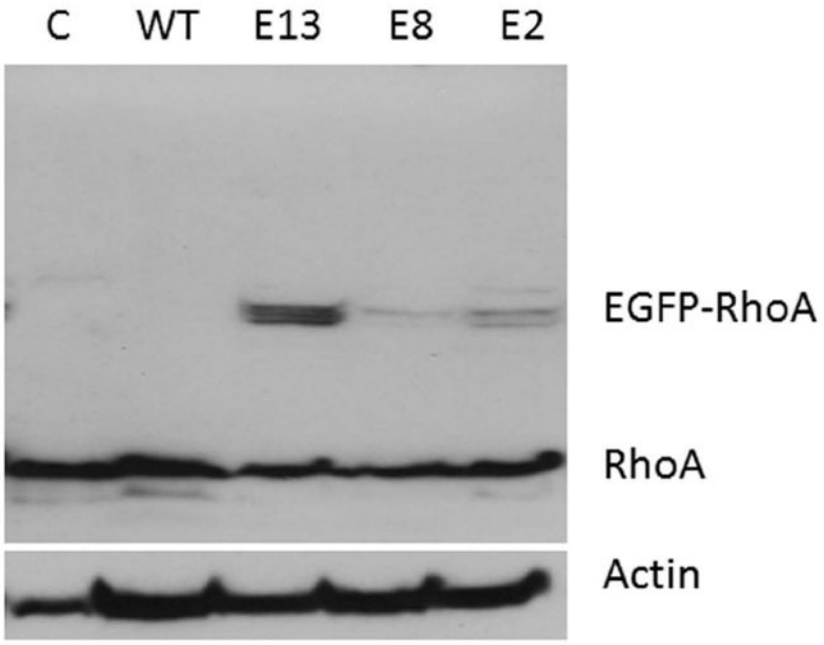

Fig. 1. Transgene expression in developing molar teeth

Western blot of extracts of first mandibular molar teeth probed with anti-RhoA antibody. Transgenic bands are visible at approximately 48 kDa for TgEGFP-RhoA^{DN}-2, 8 and 13 (E2, E8, E13) and all mice have endogenous RhoA at 22 kDa; anti-actin was used for normalization. Quantitation from two independent experiments indicated TgEGFP-RhoA^{DN}-2 (E2) expressed 35% and TgEGFP-RhoA^{DN}-8 (E8) expressed 20% of TgEGFP-RhoA^{DN}-13 (E13) transgenic protein.

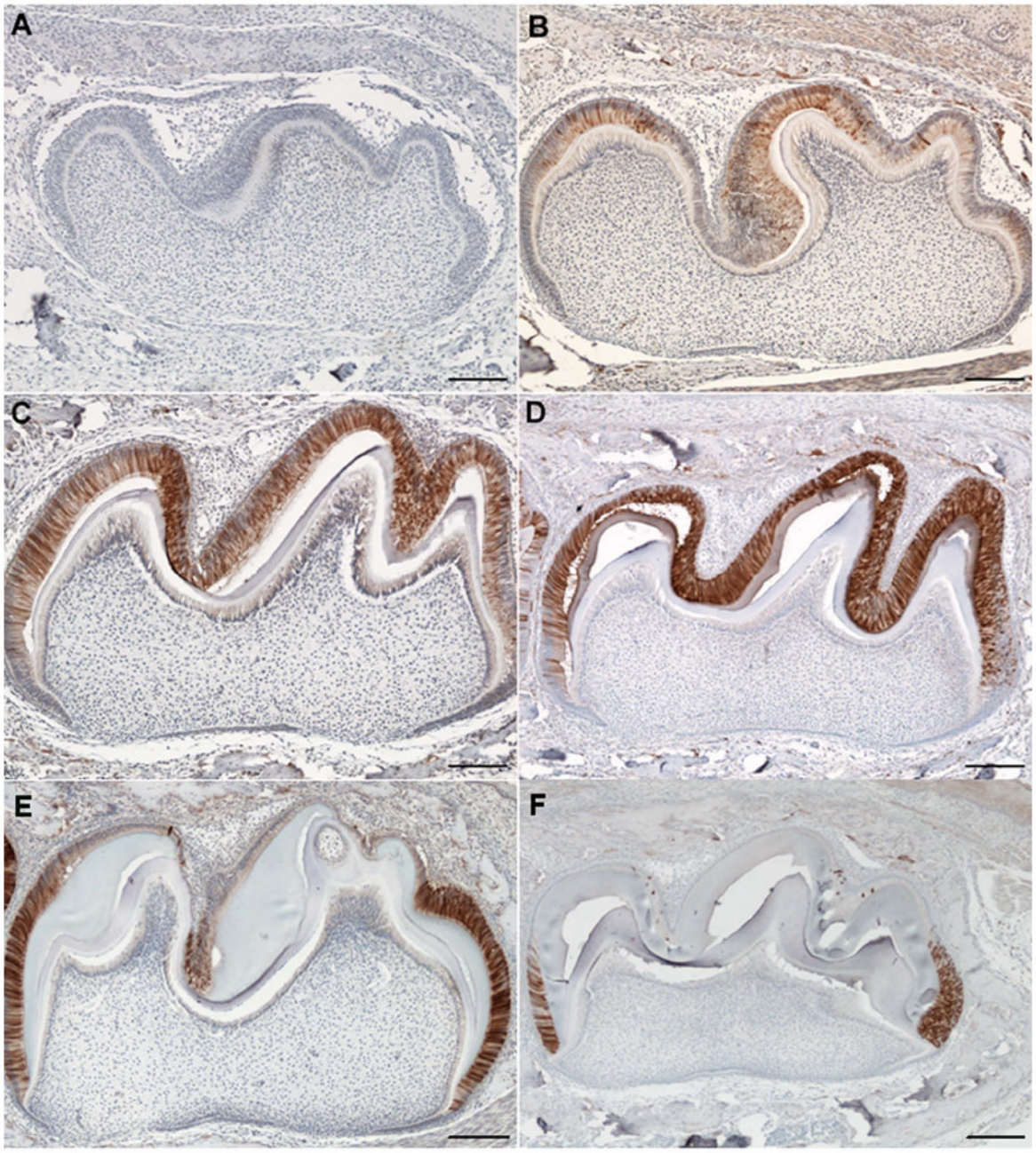

Fig. 2. Immunohistochemistry localizes transgenic protein to ameloblasts during the secretory stage of enamel development

Sections from first mandibular molars from TgEGFP-RhoA^{DN}-13 mice were incubated with anti-GFP antibody at postnatal days PN1 (A), PN2 (B), PN3 (C), PN4 (D), PN6 (E) and PN8 (F). Scale bars = 100 μm.

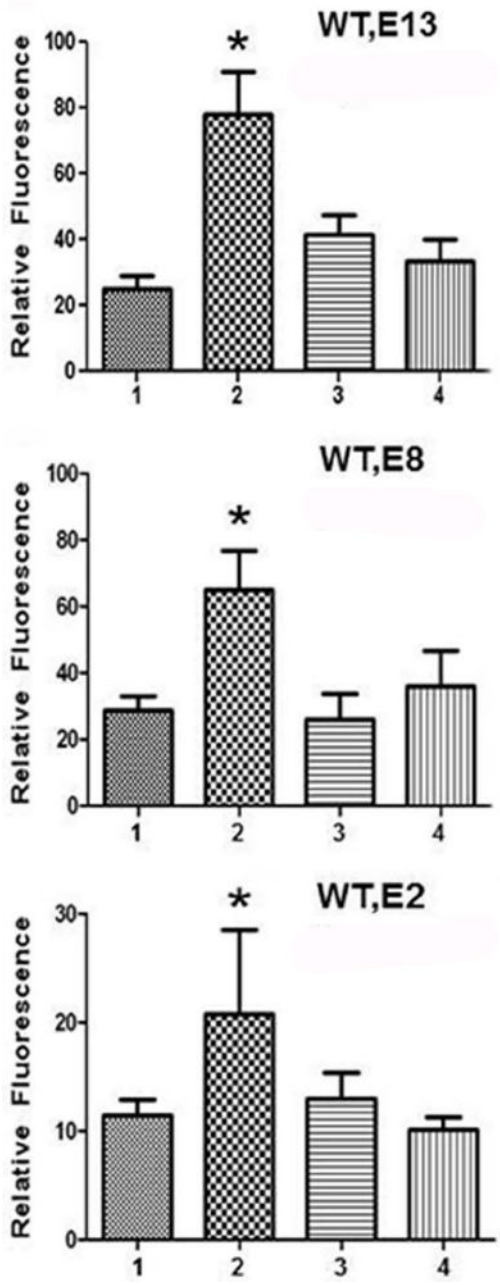

Fig. 3. Organ culture demonstrates effectiveness of the dominant negative mutation in 3 transgenic lines

First mandibular molar teeth from WT or TgEGFP-RhoA^{DN}-2, 8 or 13 (E2, E8, E13) transgenic lines were placed into organ culture and treated with 4mM NaCl or NaF for 30 min. Following phalloidin staining of sections, fluorescence relative intensities of ameloblasts were quantitated. For each comparison, bar 1: WT, NaCl; bar 2: WT, NaF; bar 3: transgenic, NaCl; bar 4: transgenic, NaF. The * indicates significant difference between WT treated with NaF and either WT treated with NaCl or transgenic treated with NaF ($P<0.0001$).

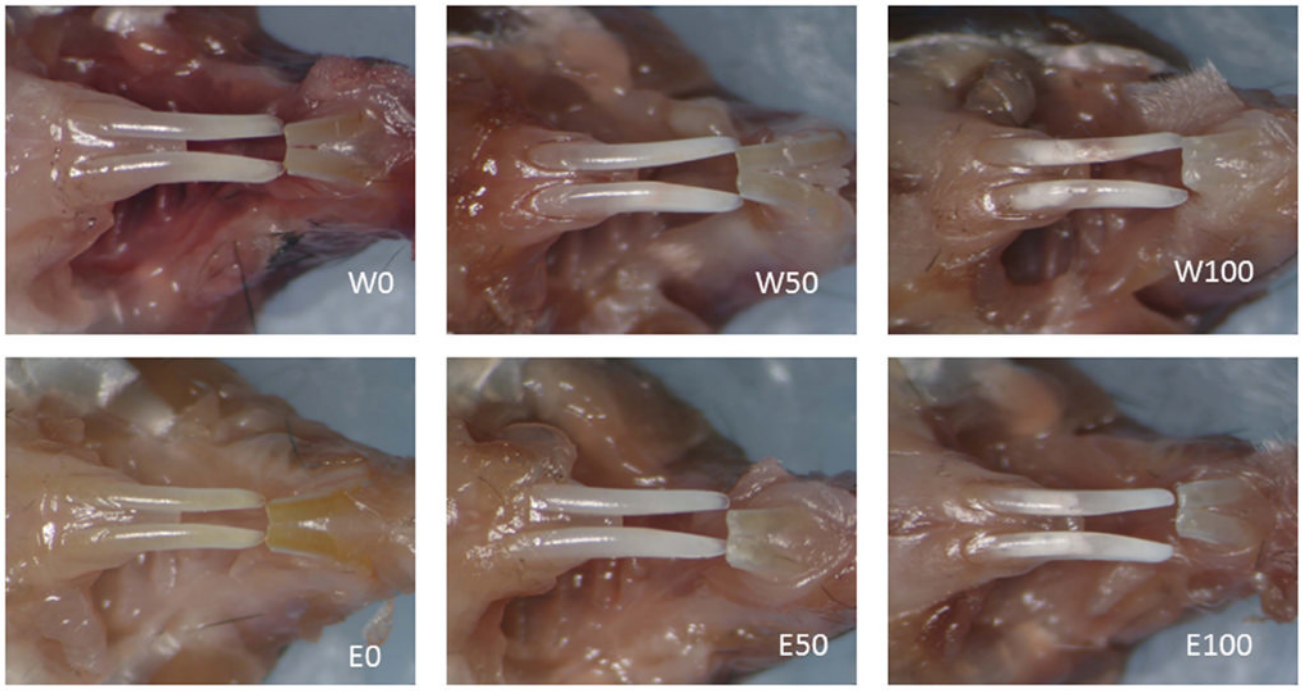

Fig. 4. Dental fluorosis assessment of incisor teeth

Clinical images of mandibular incisors. WT (W) and TgEGFP-RhoA^{DN}-13 (E) mice were provided drinking water for 4 weeks containing 0, 50 or 100 ppm F *ad libitum*.

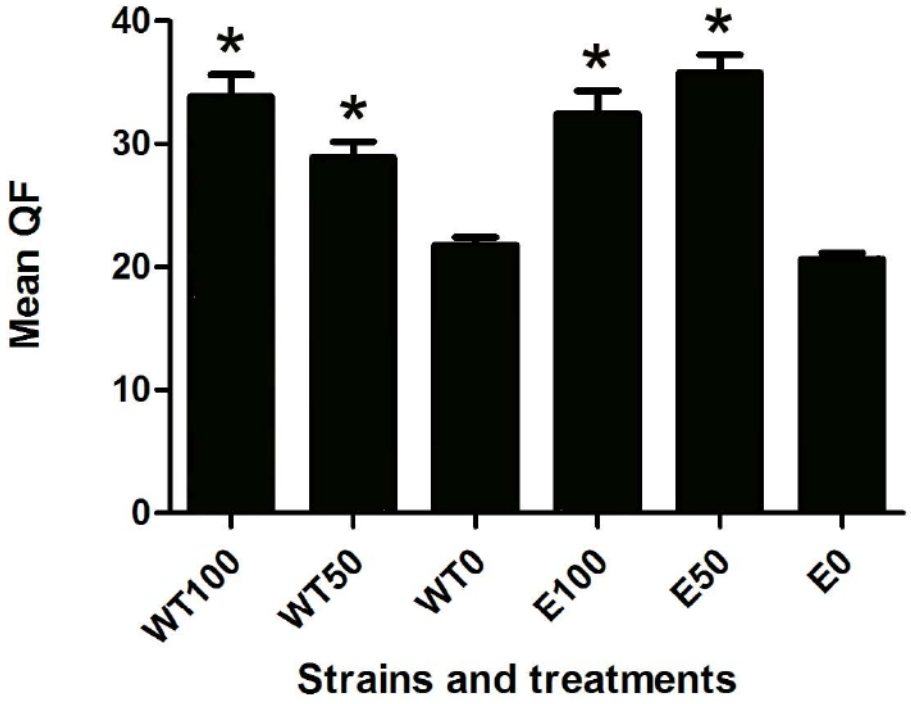

Fig. 5. Quantitative fluorescence (QF) of mandibular incisors

Results are shown for each treatment/control group and genotype shown in Fig. 4. *Results significantly different from controls.

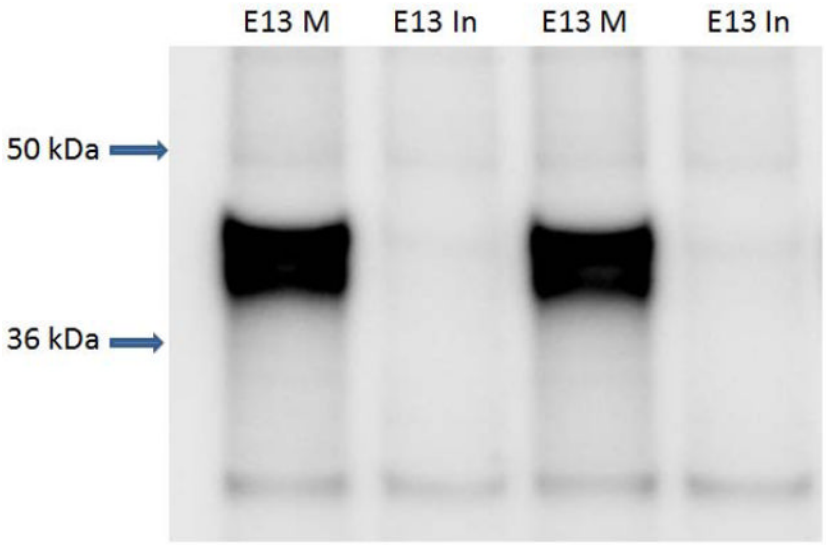

Fig. 6. Western blot to compare transgene expression in mandibular molar and incisor
Extracts of PN4 transgenic teeth (10 μg per lane) were probed with anti-GFP antibody. M: molar; In: incisor.

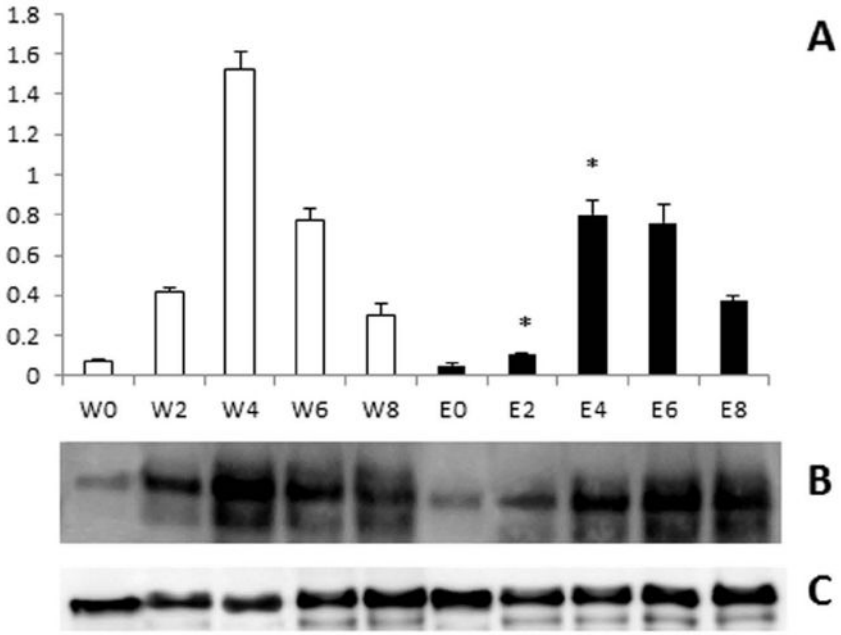

Fig. 7. Amelogenin is reduced in TgEGFP-RhoA^{DN}-13 teeth, by Western blot

A. Quantitation of normalized band intensity, where * indicates statistical difference from controls ($P<0.001$ at PN 2 and 4). W0 to W8 are PN ages for WT mice; E0 to E8 are PN ages for TgEGFP-RhoA^{DN}-13 mice. B. Western blot using anti-amelogenin antibody to detect amelogenin proteins from enamel organs from mice at the indicated ages; C. Normalization using anti-GAPDH for PN0 through PN8 for WT and transgenic mice.

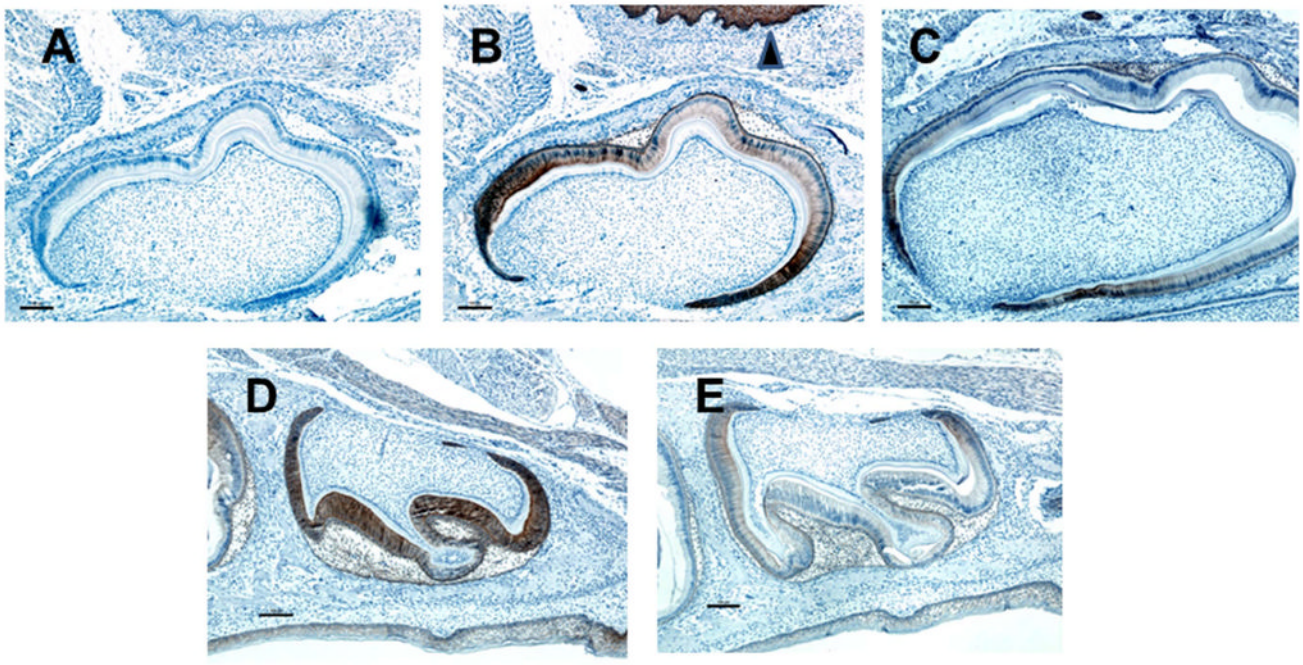

Fig. 8. E-cadherin immunostaining of ameloblasts from WT and TgEGFP-RhoA^{DN}-13 mice

Mandibular first molars (B-C) and maxillary second molars (D-E) from PN4 mice were stained with anti-E-cadherin antibody. A: First molar control lacking primary antibody; B,D: WT, anti-E-cadherin; C,E: TgEGFP-RhoA^{DN}-13, anti-E-cadherin. Scale bar = 200 μm.

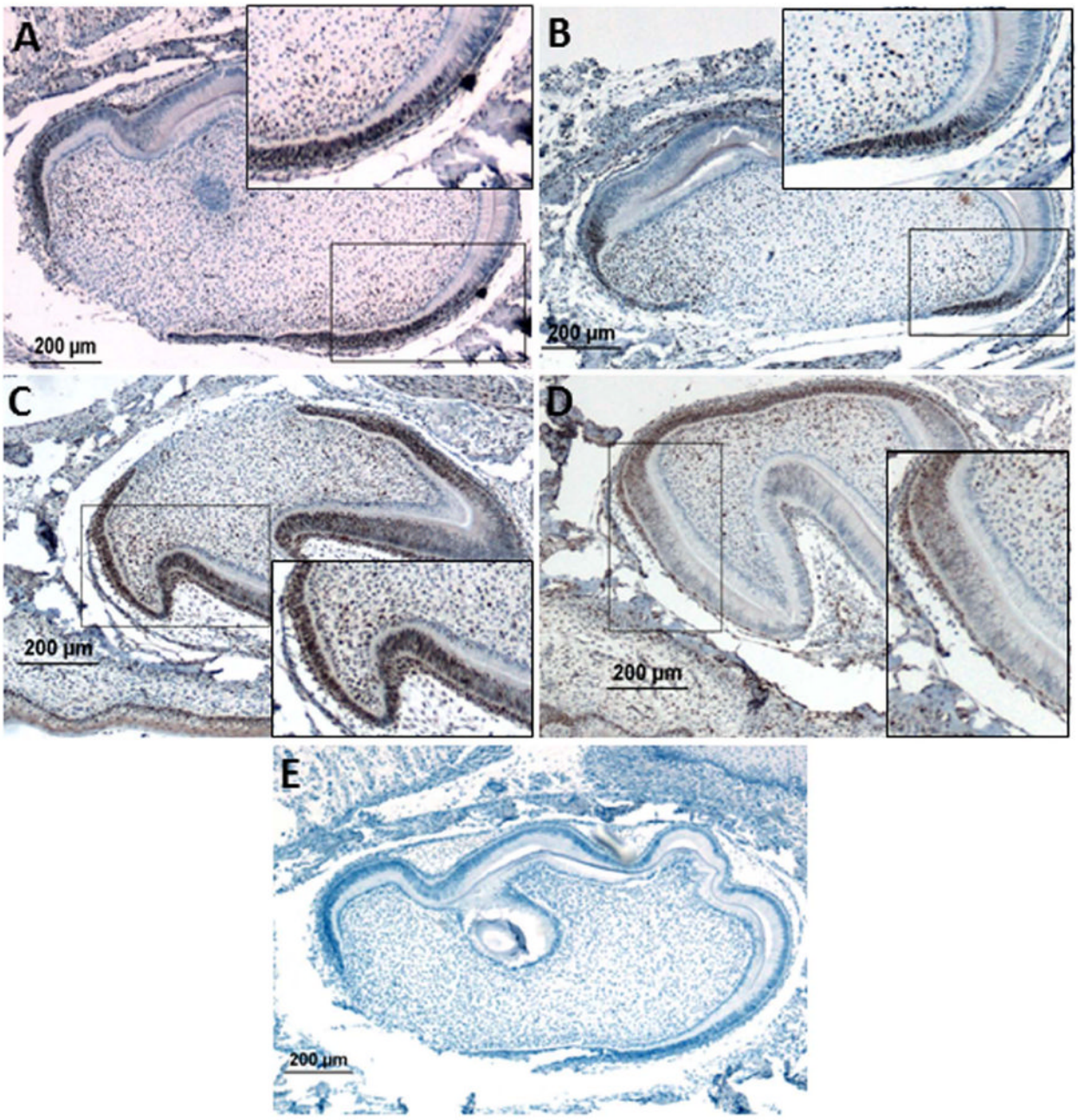

Fig. 9. Ki67 labels fewer ameloblast nuclei in TgEGFP-RhoA^{DN}-13 transgenic compared to WT first mandibular molars from mice of the same age

Mandibular PN3 (A,B,E) and maxillary PN2 (C,D) first molars. A,C: WT, anti-Ki67; B,D: TgEGFP-RhoA^{DN}-13, anti-Ki67; E: control lacking primary antibody. Dark nuclei represent Ki67 positive ameloblasts in magnified inserts. Scale bar = 200 μm.

Table

Elastic Modulus and Hardness in Molar Enamel

	WT Enamel	E13 Enamel
Elastic Modulus (GPa)	56.7 ± 17.9	49.2 ± 18.7
Hardness (GPa)	2.85 ± 1.14	3.08 ± 1.48

Legend: Nanoindentation performed in cross sections of enamel from the surface to the dentin-enamel junction of the mesial cusps of molars from 8 week old wild-type (WT) and TgEGFP-RhoA^{DN}-13 (E13) mice. n=6 independent mice with one molar per mouse measured at 20 locations.